

Research on asymmetrical supporting rotor system with radial clearance

Li Mo ¹, Liu Yongbao¹ and Wang Qiang^{1,2*}

¹College of power engineering, Naval University of Engineering, Wuhan Hubei 430033, People's Republic of China

²College of weapon engineering, Naval University of Engineering, Wuhan, Hubei 430033, People's Republic of China

Email: 572029663@qq.com

Abstract: In this paper, the dynamic model of the rotor with asymmetric support structure of ball bearing and cylindrical roller bearing is established based on the rotor support structure of a gas turbine. The influence of the radial clearance of the rolling bearing on the nonlinear dynamics of this type of rotor system is studied. The fourth-order Runge-Kutta method with variable step is adopted to analysis the dynamic characteristics of the system by using the bifurcation diagram, phase diagram, Poincaré section diagram and FFT diagram of the system. The result shows that when the radial clearance is small, the system has a long period of stability. The system will gradually exhibit nonlinear behaviors such as period 2 motion and chaotic motion with the increase of radial clearance. The research can help to reveal the nonlinear dynamic behaviors of the rotor system with radial clearance of the rolling bearing and provide some theoretical basis for the theoretical design and fault diagnosis of complex rotor system.

1. Introduction

Bearing-rotor system with rolling bearing is a typical form of mechanical structure. Rolling bearing has complex nonlinear behavior. The nonlinear is mainly reflected in the bearing radial clearance and Hertz contact force. Some scholars have studied the influence of bearing radial clearance on the rolling bearing-rotor system by using the nonlinear theory. Chen Guo, Zhang Liqin, Zhang Yaoqiang, Tiwari, SHUPANDHYAY, Chen [1-6] established the rotor system model supported by rolling bearings. The relationship between the radial clearance of the bearing and the nonlinear behavior of the rotor system is studied. Tao Hailiang, Wei Bin and Liang Mingxuan[7-9]studied the ball bearing-rotor dynamics characteristics considering the radial clearance of the bearing. Based on the Floquet theory, Bai Changqing [10] studied the relationship between the radial clearance of bearings and the stability of the periodic solution of the rotor system. Wang Haifei [11] established an integral model of aeroengine with radial clearance of rolling bearing and studied the influence of ball bearing radial clearance on the bearing stiffness. Li Hongliang[12] studied the relationship between the bearing radial clearance and rolling bearing-rotor system of the main resonance

To sum up, when studying the radial clearance of bearing, the rotor system models established by the above scholars are symmetrical support structures and the support bearings are ball bearings. However, in the actual rotating machinery such as a certain type of gas turbine compressor system rotor, the supporting structure of the rotor system is asymmetric. The system front-end support is ball bearing and the back-end support is the cylindrical roller bearing. Rotor system of this type of support structure often



fails. Therefore, it is urgent to study the nonlinear dynamic influence of bearing radial clearance on asymmetrical bearing rotor system.

2. Asymmetrical bearing-rotor dynamics model

In this paper, a rotor system model with asymmetric support is established considering the nonlinear Hertz contact force of two kinds of rolling bearings. According to the principle of Lagrange equation, a set of dynamic differential equations of an asymmetrical rolling bearing-rotor system is established.

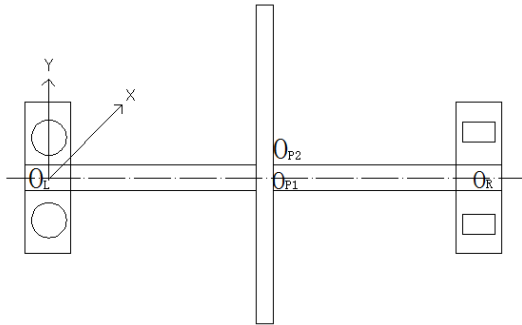


Figure 1.1 Asymmetrical bearing-rotor system model diagram

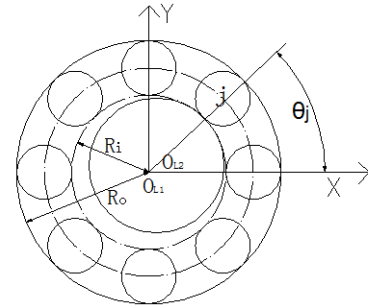


Figure 1.2 Roller bearing model diagram

$$\begin{aligned}
 m_p x_p + c_p \dot{x}_p + k_p (x_p - x_R) + k_p (x_p - x_L) &= m_p e \omega^2 \cos(\omega t) \\
 m_p y_p + c_p \dot{y}_p + k_p (y_p - y_R) + k_p (y_p - y_L) &= m_p e \omega^2 \sin(\omega t) - m_p g \\
 m_R x_R + c_R \dot{x}_R + k_p (x_R - x_p) &= F_{Rx} \\
 m_R y_R + c_R \dot{y}_R + k_p (y_R - y_p) &= F_{Ry} - m_R g \\
 m_L x_L + c_L \dot{x}_L + k_p (x_L - x_p) &= F_{Lx} \\
 m_L y_L + c_L \dot{y}_L + k_p (y_L - y_p) &= F_{Ly} - m_L g
 \end{aligned}
 \tag{1.1}$$

the bearing support force is:

$$\begin{cases}
 F_x = \sum_{j=1}^Z F_{j,x} = \sum_{j=1}^Z F_j \cos(\theta_j) = K_b \sum_{j=1}^Z H(\chi_j) \chi_j^n \cos(\theta_j) \\
 F_y = \sum_{j=1}^Z F_{j,y} = \sum_{j=1}^Z F_j \sin(\theta_j) = K_b \sum_{j=1}^Z H(\chi_j) \chi_j^n \sin(\theta_j)
 \end{cases}
 \tag{1.2}$$

where $\theta_j = \frac{R_i}{R_i + R_o} \omega t + \frac{2\pi}{Z} (Z - j)$ is the angular position of the j th rolling element,

$\chi_j = x \cos \theta_j + y \sin \theta_j - Gr$ is the contact deformation of the j th rolling element, $H(\chi_j) = \begin{cases} 1 & \chi_j > 0 \\ 0 & \chi_j \leq 0 \end{cases}$

is the function of Heaviside, n is $3/2$ when the rolling bearing is a ball bearing, and n is $10/9$ when the rolling bearing is a cylindrical roller bearing.

Table 1.1 The meaning of symbols in the equation meaning

Symbol	meaning	Symbol	meaning
m_p, c_p	mass of rotor, damping of rotor	x_p, y_p	the x and y direction displacement of rotor center
m_R, c_R	mass of ball bearing, damping of ball bearing	x_R, y_R	the x and y direction displacement of ball bearing center
m_L, c_L	mass of cylindrical roller bearing, damping of cylindrical roller bearing	x_L, y_L	the x and y direction displacement of cylindrical roller bearing center
e	eccentric distance	F_{Rx}, F_{Ry}	the x and y direction contact force of ball bearing

ω	rotating speed	F_{Lx}, F_{Ly}	the x and y direction contact force of cylindrical roller bearing
----------	----------------	------------------	---

3. Non-linear dynamic numerical simulation of asymmetrical bearing-rotor system

The parameters of the rotor are $m_p = 120\text{kg}$, $k_p = 2.5 \times 10^7 \text{N/m}$, $c_p = 1050 \text{N s/m}$ and $e = 10\mu\text{m}$. The parameters of the bearing are from the literature [13]. The detailed structural parameters are shown in Table 2.1. The varying compliance frequency (f_{VC}) of two rolling bearings are $f_{VC1} = BN_1\omega = 3.052\omega$, $f_{VC2} = BN_2\omega = 4.287\omega$. Gr is the the radial clearance of the rolling bearing.

Table 2.1 Bearing parameters

Ball bearing SKF 6204		Cylindrical roller bearing SKF NJ204ECP	
Ri(mm)	25.6	Ri(mm)	26.5
Ro(mm)	41.4	Ro(mm)	41.5
ZR	8	ZL	11
mR(kg)	2.3	mL(kg)	2.3
cR(N*s/m)	572.4	cL(N*s/m)	646
KbR(N/m)	9.21×10^9	KbL(N/m)	3.21×10^8

In this paper, the fourth order Runge-Kutta method is used to solve the nonlinear equations(1.1) numerically. The numerical result is visualized and analyzed with the phase diagram, Poincaré section diagram and FFT diagram. The abscissa of the FFT diagram is the ratio of the signal frequency and the rotation frequency, which is defined as the frequency ratio λ .

3.1 Effect of speed on the different clearance of asymmetric bearing-rotor system dynamics

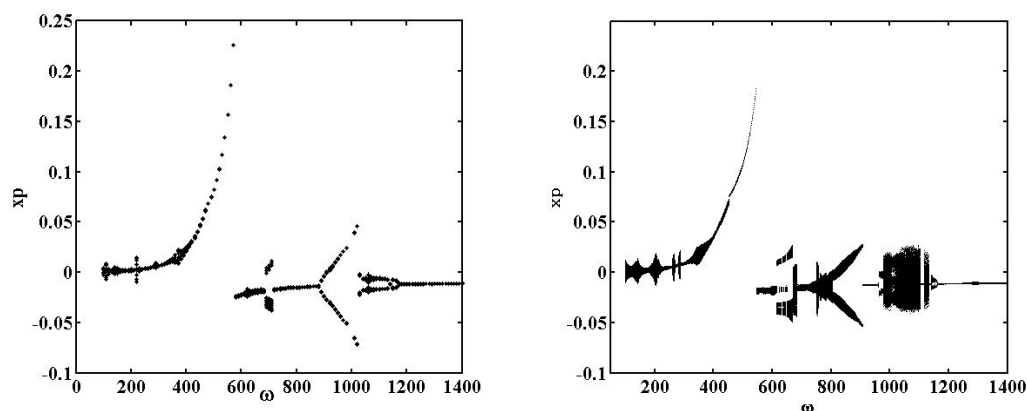


Figure 2.1 Bifurcation diagram of x_p with increasing speed:(a) $Gr=5\mu\text{m}$, (b) $Gr=20\mu\text{m}$

Figure 2.1 (a) shows the bifurcation diagram of x_p with increasing speed at $Gr=5\mu\text{m}$. It can be seen from the Figure 2.1 that the asymmetric bearing-rotor system has a strong nonlinear behavior. As the speed of the system increases, the system gradually appears the phenomenon of quasi-cycle, period 1, period 2, period 1, period 2 and period 1. There is no chaos in the whole speed range.

Because of the varying compliance of ball bearing, the varying compliance of cylindrical roller bearing and the unbalanced frequency, the three frequencies affect each other and there is a complicated frequency combination. When the rotating speed is between 100 and 453, the quasi-periodic torus bursts and reorganizes. Figure 2.2(a) is the system FFT at the speed of 100 with a maximum peak at $\lambda = 4.28$, and Figure 2.2(b) is the system FFT at the speed of 150 with a maximum peak at $\lambda = 3.05$ and two smaller peaks at $\lambda = 4.28$ and $\lambda = 1$. The system is still quasi-periodic state, which indicates that the effect of varying compliance dominates. By analyzing the FFT at the speed of 100 and 150, it is known that when the rotation speed is low, the unbalanced frequency has a little influence and the varying compliance frequency of bearing has a great influence on the rotor system. The calculation result of this paper is consistent with the conclusion of Fukata, which indicates the correctness of the asymmetric bearing-rotor

system model and the rationality of the solution.

The unbalanced force amplitude is proportional to the square of the rotation speed. As the rotation speed increases, the unbalance force amplitude increases rapidly. The system gradually performs the movement of the unbalanced frequency. The phase diagram, Poincaré section diagram, and FFT diagram of x_p at speed of 500 are shown in Figure 2.3. The phase diagram is a closed circle. The Poincaré section diagram has one isolated point and the FFT diagram shows a peak only at the unbalanced frequency.

As the speed increases, the system appears the sub-harmonics of the unbalanced frequency. Figure 2.4 is the phase diagram, Poincaré section diagram and FFT diagram of x_p at the speed of 700. There are three peaks on the FFT diagram with one-third sub-harmonics of the unbalanced frequency, two-thirds sub-harmonics of the unbalanced frequency and the unbalanced frequency.

At the speed of 710-870, one-third sub-harmonics of the unbalanced frequency and two-thirds sub-harmonics of the unbalanced frequency gradually disappear. When the speed is in the range of 870-1180, the system appears 1/2 sub-harmonics of the unbalanced frequency and the peak value of the 1/2 sub-harmonics gradually increases which results in motion of period 2. When the speed reaches at 1030, the peak value at 1/2 unbalanced frequency reaches the maximum value. Then the value suddenly decreased to less than the peak value of the balanced frequency. Figure 2.5 shows the changes of FFT diagram. At the speed of 1180-1400, the x_p changes from period 2 to period 1. Figure 2.6 shows the x_p phase diagram, Poincaré section diagram and FFT diagram at the speed of 1200.

Figure 2.1(b) is the bifurcation diagram of the x_p with the rotation speed at $Gr = 20\mu\text{m}$. With the increase of rotational speed, the system gradually appears quasi-period, period 1, period 2, chaos, period 2, period 1 phenomenon and the system leads to chaotic through period-doubling bifurcation and paroxysmal ways. Compared with the radial clearance of $5\mu\text{m}$, the system instability range increased and the motion amplitude of stability also increased significantly.

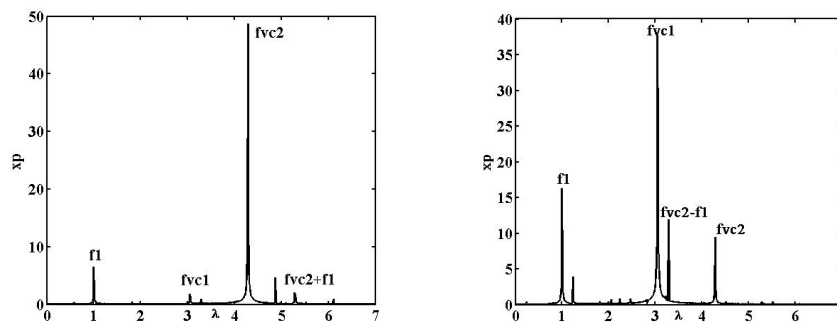


Figure 2.2 The FFT diagram: (a) $\omega=100$,(b) $\omega=150$

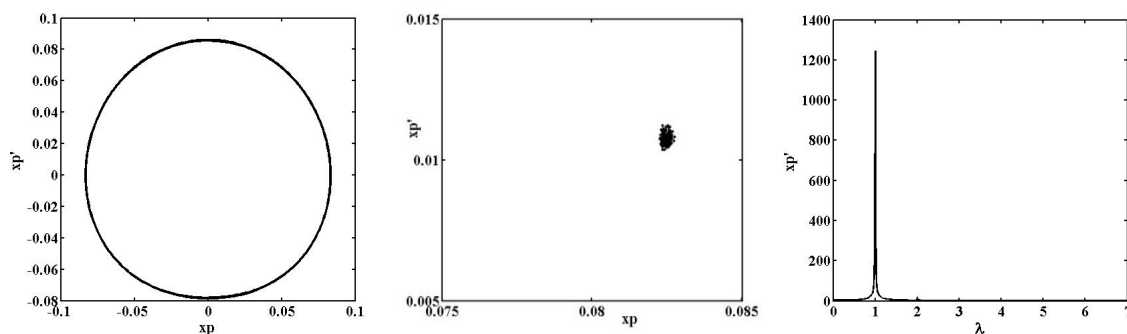


Figure 2.3 The phase diagram, Poincaré section diagram and FFT diagram of x_p at speed of 500

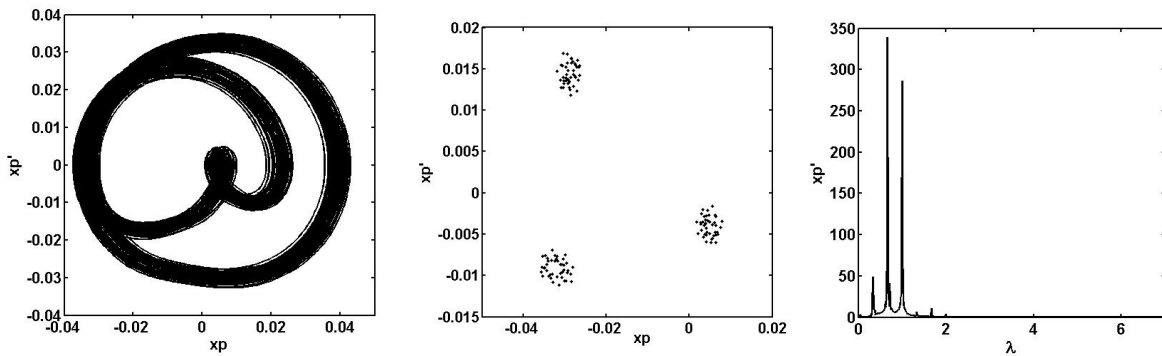


Figure 2.4 The phase diagram, Poincaré section diagram and FFT diagram of x_p at speed of 700

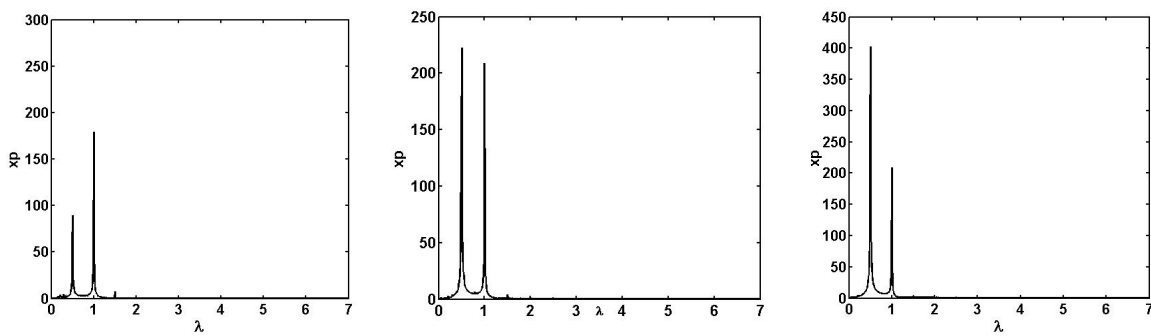


Figure 2.5 The FFT diagram : (a) $\omega=880$, (b) $\omega=910$, (c) $\omega=1080$

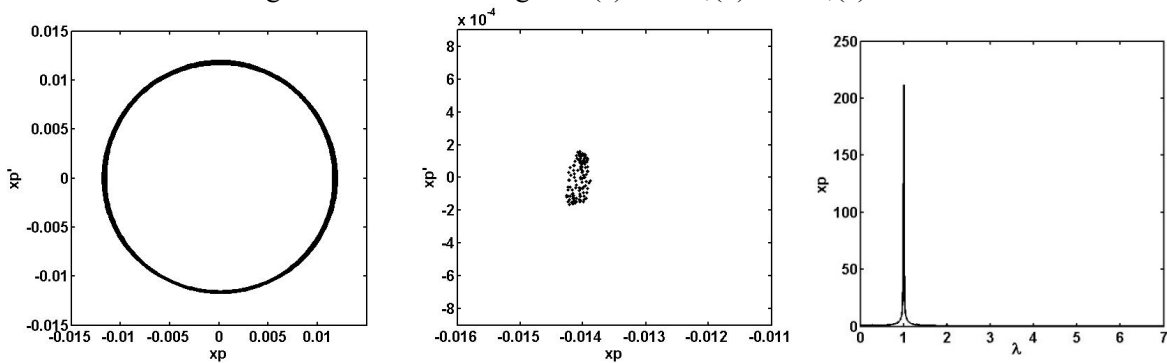


Figure 2.6 The phase diagram, Poincaré section diagram and FFT diagram of x_p at speed of 700

3.2 The bifurcation diagram with bearing radial clearance changing

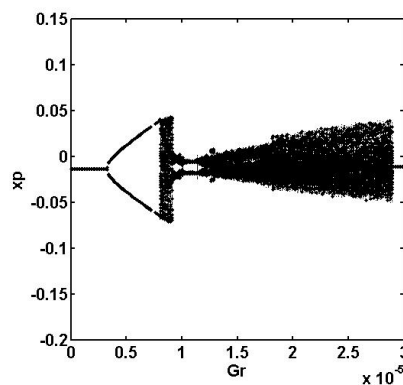


Figure 2.7 The bifurcation diagram of x_p with increasing Gr

In order to more intuitively reflect the influence of the bearing radial clearance on the rotor system,

the bifurcation diagram of x_p with the change of bearing radial clearance is calculated. The rotor system operating speed is generally greater than the first critical speed of the system. Therefore, this paper simulates the bifurcation of bearing clearance in the range of 0-30 μ m at the speed 1100. It can be seen from the Figure2.7 that with the increase of radial clearance, x_p undergoes period 1, period 2, chaotic movement, quasi-periodic, chaotic movement and period 1.

4. Conclusion

(1) There are three frequencies in the asymmetrical bearing-rotor system with varying compliance of ball bearing, varying compliance of cylindrical roller bearing and the unbalanced frequency. This is different from the symmetrical bearing rotor system. The main performance of the system is the varying compliance frequency vibration at the low speed.

(2) At the high speed, the unbalance force increases rapidly and becomes the main factor of system vibration. As the speed increases, the system appears 1/3 and 1/2 sub-harmonics. This is mainly due to the non-linear behavior caused by asymmetrical support.

(3) In the case of small bearing clearance, the asymmetrical bearing-rotor system has a strong stability and can maintain the stability even at the high speed. The bearing radial clearance can be minimized in the bearing production process. Due to the influence of friction and so on, when the rotor system runs at the operation speed for a long time, the radial clearance of the bearing will gradually increase, which results in the decrease of the stability of the system movement. Therefore the bearing should be lubricated well during the rotor operation.

References

- [1] CHEN Guo 2007. Analysis of nonlinear dynamic response of unbalanced rotor system supported on rolling bearing *China Mechanical Engineering* **18**(23):2773-2778.
- [2] Zhang Liqin 2007 Nonlinear dynamic analysis of rolling bearing-rotor system *Methods of Heavy Machinery* **01**: 20-26.
- [3] Zhang Yaoqiang 2008 Analysis of nonlinear dynamic response of rolling bearing-jetffott rotor system *Journal of Vibration and Shock* **27** (5): 56- 59.
- [4] Tiwari M,Gupta K 2000 Effect of radial internal clearance of a ball bearing on the dynamics of a balanced horizontal rotor *Journal of sound and Vibration* **238**(5):723- 756.
- [5] S.H.UPANDHYAY 2010 Analysis of nonlinear phenomena in high speed ball bearing due to radial clearance and unbalanced rotor effects *Journal of Vibration and Control* **16**(1):65-88.
- [6] Chen G 2010 Nonlinear dynamic analysis and experiment verification of rotor ball bearings support stator coupling system for aeroengine with rubbing coupling faults *Journal of Engineering for Gas Turbines and Power* **132**: 1-9.
- [7] Tao Hailiang 2013 Nonlinear dynamic response analysis of a rolling bearing-rotor system *Gas Turbine Technology* **26** (1): 15-20.
- [8] Wei Bin 2012 Analysis of dynamic characteristics of a rolling bearing-rotor system *Actaines* **(10)**: 1-6.
- [9] Liang Mingxuan 2014 Study on the vortex coupling dynamics characteristics of the rolling bearing biased rotor system *VIBRATION AND SHOC* **33** (12): 35-41
- [10] Bai Changqing 2006 Nonlinear dynamic stability of a balanced rotor system with radial internal clearance considering rolling bearing *Applied Mathematics and Mechanics* **27** (2): 159-169.
- [11] Wang Haifei 2016 Vibration response characteristics of aeroengine with radial clearance *Propulsion Technology* **37** (5): 945-959
- [12] Li Hongliang 2013 Primary resonance study of bearing-rotor system with gap ball *Acta Mechanica Sinica* **34** (6): 1356-1362.
- [13] S.H.Ghafari,F.Golnaraghi.F.Ismail. 2008 Effect of localized faults on chaotic vibration of rolling element bearing *Nonlinear Dynamic* **53**:287-301.